ACTA MECHANICA SINICA (English Series), Vol.14, No.4, Nov. 1998 ISSN 0567-7718
The Chinese Society of Theoretical and Applied Mechanics
Chinese Journal of Mechanics Press, Beijing, China
Allerton Press, INC., New York, U.S.A.

CRACK KINKING IN PIEZOELECTRIC MATERIALS*

Qin Qinghua (秦庆华)
(*Dept. of Mechanical Engineering, University of Sydney, Sydney, NSW* 2006, *Australia*)

ABSTRACT: A solution is presented for a class of two-dimensional electroelastic branched crack problems. Explicit Green's function for an interface crack subject to an edge dislocation is developed using the extended Stroh formulation allowing the branched crack problem to be expressed in terms of coupled singular integral equations. The integral equations are obtained by the method that models a kink as a continuous distribution of edge dislocations, and the dislocation density function is defined on the line of the branch crack only. Competition between crack extension along the interface and kinking into the substrate is investigated using the integral equations and the maximum energy release rate criterion. Numerical results are presented to show the effect of electric field on the path of crack extension.

KEY WORDS: piezoelectric, crack, fracture, dislocation, bimaterial

1 INTRODUCTION

Due to the intrinsic coupling effect between electrical and mechanical fields, piezoelectric materials have been widely used as electromechanical devices in which interfaces between materials are ubiquitous. As such, the interfacial failure mechanism has caused researchers to devote a great deal of attention to study the selection of crack path. Generally fracture along and adjacent to bimaterial interfaces has several morphological manifestations. In some cases the fracture occurs at the interface, while in others fracture occurs in the more brittle constituent[1]. Various hypotheses have been made concerning the crack kinking both in homogeneous material and bimaterials[2~4], such as maximum energy release rate[3], the minimum strain energy density theory[2]. In this context, there are many analytical studies of crack kinking by using the above criteria, e.g, the work of Lo[5]; Hayashi and Nemat-Nasser[3,6], He and Hutchinson[7]; Miller and Stock[8]; Hutchinson and Suo[9]; Wang et al.[10]; Atkinson et al.[11], and others.

The present paper deals with the problems of crack kinking in piezoelectric bimaterials. The focus is on the effect of electric field on the path selection of crack extension. The geometrical configuration analyzed is depicted in Fig.1. A main crack of length $2c$ is shown lying along the interface between the two dissimilar piezoelectric materials, with a branch of length a and angle θ kinks upward into material 1. The length a is assumed to be small compared to the length $2c$ of the main crack. To solve the branch problem, we first derive the Green's function satisfying the traction-charge free conditions on the main crack by way

Received 8 May 1998
* The work was supported by the Australian Research Council through a Queen Elizabeth II fellowship and by the Australian Academy of Science through the J.G. Russell Award.

of the Stroh formulation and the solution for bimaterials due to an edge dislocation. The resulting singular integral equations for the dislocation density functions are, then, defined on the line of the branch only, which are solved numerically. Competition between crack extension along the interface and kinking into the substrate is investigated with the aid of the integral equations and the maximum energy release rate criterion. The formulation for the energy release rate and the stress and electric displacement (SED) intensity factors to the onset of kinking are expressed in terms of dislocation density function and branch angle. The numerical results for the energy release rate vs loading condition and branch angle are presented to demonstrate the relationship among the kinking angle, loading condition (the ratio of $\sigma_{22}^{\infty}/D_2^{\infty}$) and the energy release rate.

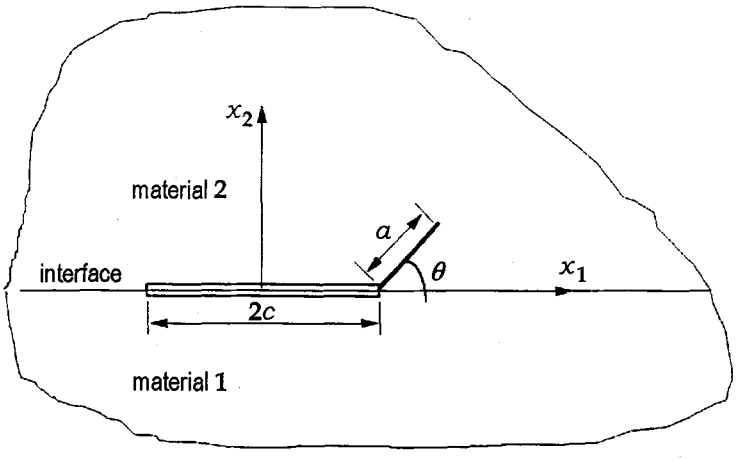

Fig.1 Geometry of the kinked crack system

2 PROBLEM FORMULATION

2.1 Stroh's Formulation

Based upon Stroh's formulism[12] in anisotropic elasticity, the general solutions for the uncoupled steady-state plane piezoelectricity has been presented by Barnett and Lothe[13] as

$$\boldsymbol{u} = 2\mathrm{Re}[\boldsymbol{A}\boldsymbol{f}(z)] \qquad \boldsymbol{\phi} = 2\mathrm{Re}[\boldsymbol{B}\boldsymbol{f}(z)] \qquad \Pi_1 = -\boldsymbol{\phi}_{,2} \qquad \Pi_2 = \boldsymbol{\phi}_{,1} \tag{1}$$

where

$$\boldsymbol{f}(z) = \{f_1(z_1)\ f_2(z_2)\ f_3(z_3)\ f_4(z_4)\}^{\mathrm{T}} \qquad z_i = x_1 + p_i x_2 \tag{2}$$

(x_1, x_2) is a fixed rectangular coordinate system, overbar denotes the complex conjugate, a comma followed by an argument (or a prime later) represents the differentiation with respect its argument, Re stands for the real part of a complex number, $\boldsymbol{u} = \{u_1\ u_2\ u_3\ \varphi\}^{\mathrm{T}}$, $\Pi_j = \{\sigma_{1j}\ \sigma_{2j}\ \sigma_{3j}\ D_j\}^{\mathrm{T}}$, $j = 1, 2$; $i = \sqrt{-1}$, u_i and φ are the elastic displacement and electric potential (EDEP), σ_{ij} and D_i are stress and electric displacement, p_i are the electroelastic eigenvalues of the material whose imaginary parts are positive, $\boldsymbol{A}$ and $\boldsymbol{B}$ are well-defined in the literature (see Ref.[14~16], for example), $f_i(z_i)$ are arbitrary functions with complex arguments z_i. Following the one-complex-variable approach given by Suo[17], introduce a vector function

$$\boldsymbol{f}(z) = \{f_1(z)\ f_2(z)\ f_3(z)\ f_4(z)\}^{\mathrm{T}} \qquad z = x + py \qquad \mathrm{Im}(p) > 0 \tag{3}$$

The solution to any given boundary value problem can be expressed in terms of such a vector, regardless of the precise value of p[18]. Once a solution of $\boldsymbol{f}(z)$ is obtained, the variable z in $f_i(z)$ should be replaced with the argument z_i, to compute the related fields. This approach allows the standard matrix algebra to be used in conjunction with the techniques of analytic functions of one variable, and thus bypass some complexities arising from the use of four complex variables.

2.2 Crack-Dislocation Interaction in a Homogeneous Material

Consider the problem of piezoelectric branched crack in a two-dimensional infinite medium (see Fig.1). The interaction between crack and dislocation can be analyzed by first studying the Green function due to a dislocation line since a crack may be viewed as a continuous distribution of dislocation singularities. For the infinite plane subject to a line dislocation, say $\boldsymbol{b}$, located at $z_0(x_{10}, x_{20})$, the electroelastic solution is[19]

$$\boldsymbol{f}_0(z) = \frac{\ln(z - z_0)}{2\pi i}\boldsymbol{B}^{\mathrm{T}}\boldsymbol{b} \tag{4}$$

The expression for $\boldsymbol{f}_0(z)$ is obtained by imposing zero net traction-charge in a circuit around the dislocation, and by demanding that the jumps in EDEP be given by $\boldsymbol{b} = \{\Delta u_1\ \Delta u_2\ \Delta u_3\ \Delta\varphi\}^{\mathrm{T}}$, where Δu is the jump for the quantity u across the dislocation line. In the presence of crack, however, the solution for an edge dislocation is no longer given by $\boldsymbol{f}_0(z)$ alone. In addition to the conditions imposed at z_0, the boundary conditions for the crack have to be satisfied. This can be accomplished by evaluating the traction-charge on crack face due to the dislocation singularity and introducing an appropriate function $\boldsymbol{f}_I(z)$ to cancel the traction-charge. Substituting $\boldsymbol{f}_0(z)$ from Eq.(4) into Eq.(1), the SED on the crack surface induced by the edge dislocation alone at z_0 is of the form

$$\boldsymbol{t}(x) = \boldsymbol{B}\boldsymbol{f}_0'(x) + \bar{\boldsymbol{B}}\overline{\boldsymbol{f}_0'(x)} = \frac{1}{2\pi\mathrm{i}}\boldsymbol{B}\Big\langle\frac{1}{x - z_{0\alpha}}\Big\rangle\boldsymbol{B}^{\mathrm{T}}\boldsymbol{b} - \frac{1}{2\pi\mathrm{i}}\bar{\boldsymbol{B}}\Big\langle\frac{1}{x - \bar{z}_{0\alpha}}\Big\rangle\bar{\boldsymbol{B}}^{\mathrm{T}}\boldsymbol{b} = -\boldsymbol{p}(x) \tag{5}$$

where $\Big\langle(\ )_\alpha\Big\rangle = \mathrm{diag}[(\ )_1(\ )_2(\ )_3(\ )_4]$. The prescribed traction-charge, $\boldsymbol{p}(x_1)$, leads to the following Hilbert problem[20]

$$\boldsymbol{B}\boldsymbol{f}_I'(z) = \frac{\chi(z)}{2\pi\mathrm{i}}\int_{-c}^{c}\frac{\boldsymbol{p}(x)\mathrm{d}x}{\chi^+(x)(x - z)} + \boldsymbol{c}\chi(z) \tag{6}$$

where $\chi(z)$ is the basic Plemelj function defined as

$$\chi(z) = (z^2 - c^2)^{-1/2} \tag{7}$$

Using contour integration, we finally obtain

$$\boldsymbol{f}_I'(z) = -\frac{1}{2\pi\mathrm{i}}\boldsymbol{F}_*(z, z_0)\boldsymbol{B}^{\mathrm{T}}\boldsymbol{b} + \frac{1}{2\pi\mathrm{i}}\boldsymbol{B}^{-1}\bar{\boldsymbol{B}}\boldsymbol{F}_*(z, \bar{z}_0)\bar{\boldsymbol{B}}^{\mathrm{T}}\boldsymbol{b} \qquad \boldsymbol{c} = -\frac{\boldsymbol{L}\boldsymbol{b}}{4\pi} \tag{8}$$

where

$$\boldsymbol{L} = -2\mathrm{i}\boldsymbol{B}\boldsymbol{B}^{\mathrm{T}} \qquad \boldsymbol{F}_*(z, z_0) = \frac{1}{2}\Big\langle\frac{1}{z_\alpha - z_{0\alpha}}\Big[1 - \frac{\chi(z_\alpha)}{\chi(z_{0\alpha})}\Big]\Big\rangle \tag{9}$$

The functions defined in Eqs.(4) and (8) together provide a Green's function for the crack problem

$$\boldsymbol{f}'(z) = \boldsymbol{f}_0'(z) + \boldsymbol{f}_I'(z) = \frac{1}{2\pi\mathrm{i}}\Big\{\Big[\Big\langle\frac{1}{z_\alpha - z_{0\alpha}}\Big\rangle - \boldsymbol{F}_*(z, z_0)\Big]\boldsymbol{B}^{\mathrm{T}}\boldsymbol{b} + \boldsymbol{B}^{-1}\bar{\boldsymbol{B}}\boldsymbol{F}_*(z, \bar{z}_0)\bar{\boldsymbol{B}}^{\mathrm{T}}\boldsymbol{b}\Big\} \tag{10}$$

It is obvious that the singularity is contained in $\boldsymbol{f}_0(z)$ and the crack interactions are accounted for by $\boldsymbol{f}_I(z)$.

2.3 Crack-Dislocation Interaction in a Bimaterial

Consider a crack lying along the interface between material 1 and material 2 (see Fig.1), subject to a line dislocation at $z_0(x_{10}, x_{20})$. For convenience, we assume that z_0 be in material 1. The treatment for z_0 located in material 2 requires only a slight modification. The electroelastic solution for the bimaterial due to the dislocation, $\boldsymbol{b}$, can be found in[21]

$$\boldsymbol{f}_0^{(1)}(z^{(1)}) = \frac{1}{2\pi \mathrm{i}}\Big\langle \ln(z_\alpha^{(1)} - z_{0\alpha}^{(1)})\Big\rangle \boldsymbol{B}_1^{\mathrm{T}}\boldsymbol{b} + \sum_{k=1}^{4}\Big\langle \ln(z_\alpha^{(1)} - \bar{z}_{0k}^{(1)})\Big\rangle \boldsymbol{B}^*\boldsymbol{I}_k\bar{\boldsymbol{B}}_1^{\mathrm{T}}\boldsymbol{b} \tag{11}$$

for material 1 ($x_2 = y > 0$), and

$$\boldsymbol{f}_0^{(2)}(z^{(2)}) = \sum_{k=1}^{4}\Big\langle \ln(z_\alpha^{(2)} - z_{0k}^{(1)})\Big\rangle \boldsymbol{B}_k^{**}\boldsymbol{b} \tag{12}$$

for material 2 ($y < 0$), where the superscripts $^{(1)}$ and $^{(2)}$ (or subscripts $_1$ and $_2$ below) label the quantities relating to the material 1 and 2, respectively, $\boldsymbol{I}_k = \mathrm{diag}[\delta_{1k}\ \delta_{2k}\ \delta_{3k}\ \delta_{4k}]$, $\delta_{ij} = 1$ for $i = j$; $\delta_{ij} = 0$ for $i \neq j$, and

$$\left.\begin{aligned} \boldsymbol{B}^* &= \boldsymbol{B}_1^{-1}[\boldsymbol{I} - 2(\boldsymbol{M}_1^{-1} + \bar{\boldsymbol{M}}_2^{-1})^{-1}\boldsymbol{L}_1^{-1}] \\ \boldsymbol{B}_k^{**} &= \frac{1}{2\pi \mathrm{i}}\boldsymbol{B}_2^{-1}(\bar{\boldsymbol{M}}_1^{-1} + \boldsymbol{M}_2^{-1})^{-1}\boldsymbol{L}_1^{-1}\boldsymbol{B}_1\boldsymbol{I}_k\boldsymbol{B}_1^{\mathrm{T}} \\ \boldsymbol{M}_j &= -\mathrm{i}\boldsymbol{B}_j\boldsymbol{A}_j^{-1} \qquad (j = 1, 2) \end{aligned}\right\} \tag{13}$$

the interface SED induced by the dislocation $\boldsymbol{b}$ is, then, of the form

$$\boldsymbol{t}(x) = \boldsymbol{B}_2\boldsymbol{f}_0^{'(2)}(x) + \bar{\boldsymbol{B}}_2\bar{\boldsymbol{f}}_0^{'(2)}(x) = [\boldsymbol{F}_{**}(x) + \bar{\boldsymbol{F}}_{**}(x)]\boldsymbol{b} \tag{14}$$

where

$$\boldsymbol{F}_{**}(x) = \sum_{k=1}^{4}\frac{\boldsymbol{B}_2\boldsymbol{B}_k^{**}}{x - z_{0k}^{(1)}} \tag{15}$$

This traction-charge vector, $\boldsymbol{t}(x)$ can be removed by superposing a solution with the traction-charge, $-\boldsymbol{t}(x)$, induced by the potential $\boldsymbol{f}_I(z)$. The solution for $\boldsymbol{f}_I(z)$ can be obtained by setting

$$\boldsymbol{h}(z) = \begin{cases} \boldsymbol{B}_1\boldsymbol{f}_I^{'(1)}(z) & \text{in material 1} \\ \boldsymbol{H}^{-1}\bar{\boldsymbol{H}}\boldsymbol{B}_2\boldsymbol{f}_I^{'(2)}(z) & \text{in material 2} \end{cases} \tag{16}$$

where $\boldsymbol{H} = -\boldsymbol{M}_1 - \bar{\boldsymbol{M}}_2$.

The function $\boldsymbol{h}(z)$ defined above together with prescribed traction-charge, $-\boldsymbol{t}(x_1)$, on crack faces, yields the following non-homogeneous Hilbert problem

$$\boldsymbol{h}^+(x) + \bar{\boldsymbol{H}}^{-1}\boldsymbol{H}\boldsymbol{h}^-(x) = -\boldsymbol{t}(x) \tag{17}$$

The quantities, $\boldsymbol{h}(x)$ and $\boldsymbol{t}(x)$ can be written in their components in the sense of the eigenvector $\boldsymbol{w}, \boldsymbol{w}_3$ and $\boldsymbol{w}_4$ as[18]

$$\left.\begin{aligned} \boldsymbol{h}(x) &= h_1(x)\boldsymbol{w} + h_2(x)\bar{\boldsymbol{w}} + h_3(x)\boldsymbol{w}_3 + h_4(x)\boldsymbol{w}_4 \\ \boldsymbol{t}(x) &= t(x)\boldsymbol{w} + \bar{t}(x)\boldsymbol{w} + t_3(x)\boldsymbol{w}_3 + t_4(x)\boldsymbol{w}_4 \end{aligned}\right\} \tag{18}$$

One obtains

$$\left.\begin{aligned}
h_1(z) &= -\frac{\chi(z)}{2\pi \mathrm{i}}\int_{-c}^{c}\frac{t(x)\mathrm{d}x}{\chi^+(x)(x-z)} + c_1\chi(z)\\
h_2(z) &= -\frac{\chi(z)}{2\pi \mathrm{i}}\int_{-c}^{c}\frac{\bar{t}(x)\mathrm{d}x}{\bar{\chi}^+(x)(x-z)} + c_2\chi(z)\\
h_3(z) &= -\frac{\chi_3(z)}{2\pi \mathrm{i}}\int_{-c}^{c}\frac{t_3(x)\mathrm{d}x}{\chi_3^+(x)(x-z)} + c_3\chi(z)\\
h_4(z) &= -\frac{\chi_4(z)}{2\pi \mathrm{i}}\int_{-c}^{c}\frac{t_4(x)\mathrm{d}x}{\chi_4^+(x)(x-z)} + c_4\chi(z)
\end{aligned}\right\} \tag{19}$$

where $\boldsymbol{w}, \boldsymbol{w}_3$ and $\boldsymbol{w}_4$ are eigenvectors and have been defined in [18], and

$$\left.\begin{aligned}
\chi(z) &= (z+c)^{-1/2-\mathrm{i}\varepsilon}(z-c)^{-1/2+\mathrm{i}\varepsilon}\\
\chi_3(z) &= (z+c)^{-1/2-\kappa}(z-c)^{-1/2+\kappa}\\
\chi_4(z) &= (z+c)^{-1/2+\kappa}(z-c)^{-1/2-\kappa}
\end{aligned}\right\} \tag{20}$$

and the functions h_i and t_i are evaluated by taking inner products with $\boldsymbol{w}, \boldsymbol{w}_3$ and $\boldsymbol{w}_4$, respectively, i.e.

$$\left.\begin{aligned}
&h_1(x) = \frac{\bar{\boldsymbol{w}}^{\mathrm{T}}\boldsymbol{H}\boldsymbol{h}(x)}{\bar{\boldsymbol{w}}^{\mathrm{T}}\boldsymbol{H}\boldsymbol{w}} \qquad h_2(x) = \frac{\boldsymbol{w}^{\mathrm{T}}\boldsymbol{H}\boldsymbol{h}(x)}{\boldsymbol{w}^{\mathrm{T}}\boldsymbol{H}\bar{\boldsymbol{w}}}\\
&h_3(x) = \frac{\boldsymbol{w}_4^{\mathrm{T}}\boldsymbol{H}\boldsymbol{h}(x)}{\boldsymbol{w}_4^{\mathrm{T}}\boldsymbol{H}\boldsymbol{w}_3} \qquad h_4(x) = \frac{\boldsymbol{w}_3^{\mathrm{T}}\boldsymbol{H}\boldsymbol{h}(x)}{\boldsymbol{w}_3^{\mathrm{T}}\boldsymbol{H}\bar{\boldsymbol{w}}_4}\\
&t = \frac{\bar{\boldsymbol{w}}^{\mathrm{T}}\boldsymbol{H}\boldsymbol{t}(x)}{\bar{\boldsymbol{w}}^{\mathrm{T}}\boldsymbol{H}\boldsymbol{w}} \qquad t_3 = \frac{\bar{\boldsymbol{w}}_4^{\mathrm{T}}\boldsymbol{H}\boldsymbol{t}(x)}{\bar{\boldsymbol{w}}_4^{\mathrm{T}}\boldsymbol{H}\boldsymbol{w}_3} \qquad t_4 = \frac{\bar{\boldsymbol{w}}_3^{\mathrm{T}}\boldsymbol{H}\boldsymbol{t}(x)}{\bar{\boldsymbol{w}}_3^{\mathrm{T}}\boldsymbol{H}\boldsymbol{w}_4}
\end{aligned}\right\} \tag{21}$$

The contour integration of Eq.(19) provides

$$h_i(z) = \boldsymbol{h}_i^*(z)\cdot\boldsymbol{b} \qquad (i=1,2,3,4) \tag{22}$$

$$\boldsymbol{h}_1^*(z) = \frac{\bar{\boldsymbol{w}}^{\mathrm{T}}\boldsymbol{H}}{\bar{\boldsymbol{w}}^{\mathrm{T}}\boldsymbol{H}\boldsymbol{w}}\sum_{k=1}^{4}\left[\boldsymbol{F}(\varepsilon,\chi,z,z_{0k}^{(1)},\boldsymbol{B}_2,\boldsymbol{B}_k^{**}) + \boldsymbol{F}(\varepsilon,\chi,z,\bar{z}_{0k}^{(1)},\bar{\boldsymbol{B}}_2,\bar{\boldsymbol{B}}_k^{**})\right] \tag{23}$$

$$\boldsymbol{h}_2^*(z) = \frac{\boldsymbol{w}^{\mathrm{T}}\boldsymbol{H}}{\boldsymbol{w}^{\mathrm{T}}\boldsymbol{H}\bar{\boldsymbol{w}}}\sum_{k=1}^{4}\left[\boldsymbol{F}(-\varepsilon,\bar{\chi},z,z_{0k}^{(1)},\boldsymbol{B}_2,\boldsymbol{B}_k^{**}) + \boldsymbol{F}(-\varepsilon,\bar{\chi},z,\bar{z}_{0k}^{(1)},\bar{\boldsymbol{B}}_2,\bar{\boldsymbol{B}}_k^{**})\right] \tag{24}$$

$$\boldsymbol{h}_3^*(z) = \frac{\boldsymbol{w}_4^{\mathrm{T}}\boldsymbol{H}}{\boldsymbol{w}_4^{\mathrm{T}}\boldsymbol{H}\boldsymbol{w}_3}\sum_{k=1}^{4}\left[\boldsymbol{F}(-\mathrm{i}\kappa,\chi_3,z,z_{0k}^{(1)},\boldsymbol{B}_2,\boldsymbol{B}_k^{**}) + \boldsymbol{F}(-\mathrm{i}\kappa,\chi_3,z,\bar{z}_{0k}^{(1)},\bar{\boldsymbol{B}}_2,\bar{\boldsymbol{B}}_k^{**})\right] \tag{25}$$

$$\boldsymbol{h}_4^*(z) = \frac{\boldsymbol{w}_3^{\mathrm{T}}\boldsymbol{H}}{\boldsymbol{w}_3^{\mathrm{T}}\boldsymbol{H}\boldsymbol{w}_4}\sum_{k=1}^{4}\left[\boldsymbol{F}(\mathrm{i}\kappa,\chi_4,z,z_{0k}^{(1)},\boldsymbol{B}_2,\boldsymbol{B}_k^{**}) + \boldsymbol{F}(\mathrm{i}\kappa,\chi_4,z,\bar{z}_{0k}^{(1)},\bar{\boldsymbol{B}}_2,\bar{\boldsymbol{B}}_k^{**})\right] \tag{26}$$

$$\left.\begin{aligned}
&c_1 = -\frac{\bar{\boldsymbol{w}}^{\mathrm{T}}\boldsymbol{H}}{\bar{\boldsymbol{w}}^{\mathrm{T}}\boldsymbol{H}\boldsymbol{w}}\frac{\boldsymbol{X}_*}{1+\mathrm{e}^{-2\pi\varepsilon}} \qquad c_2 = -\frac{\boldsymbol{w}^{\mathrm{T}}\boldsymbol{H}}{\boldsymbol{w}^{\mathrm{T}}\boldsymbol{H}\bar{\boldsymbol{w}}}\frac{\boldsymbol{X}_*}{1+\mathrm{e}^{2\pi\varepsilon}}\\
&c_3 = -\frac{\boldsymbol{w}_4^{\mathrm{T}}\boldsymbol{H}}{\boldsymbol{w}_4^{\mathrm{T}}\boldsymbol{H}\boldsymbol{w}_3}\frac{\boldsymbol{X}_*}{1+\mathrm{e}^{2\mathrm{i}\pi\kappa}} \qquad c_4 = -\frac{\boldsymbol{w}_3^{\mathrm{T}}\boldsymbol{H}}{\boldsymbol{w}_3^{\mathrm{T}}\boldsymbol{H}\bar{\boldsymbol{w}}_4}\frac{\boldsymbol{X}_*}{1+\mathrm{e}^{-2\mathrm{i}\pi\kappa}}
\end{aligned}\right\} \tag{27}$$

where

$$\boldsymbol{F}(r,\chi,z,z_{0k},\boldsymbol{X},\boldsymbol{Y}) = -\frac{\boldsymbol{XY}}{(1+\mathrm{e}^{-2\pi r})}\Big[1-\frac{\chi(z)}{\chi(z_{0k})}\Big]\frac{1}{z-z_{0k}}$$
$$\boldsymbol{X}_* = \sum_{k=1}^{4}(\boldsymbol{B}_2\boldsymbol{B}_k^{**}+\bar{\boldsymbol{B}}_2\bar{\boldsymbol{B}}_k^{**})\boldsymbol{b} \tag{28}$$

Once $h_i(z)$ has been obtained, the functions $\boldsymbol{f}_I'^{(j)}(z)$ can be evaluated through the use of Eqs.(16) and (18).

It should be pointed out that the above solutions do not apply when the dislocation is located at the interface. For an edge dislocation $\boldsymbol{b}$ located at the interface, say x_0, the solution can be obtained by setting

$$\left.\begin{aligned} \boldsymbol{f}_0^{(1)}(z) &= \langle \ln(z_\alpha^{(1)}-x_0)\rangle \boldsymbol{q}_1 && \text{for } y>0 \\ \boldsymbol{f}_0^{(2)}(z) &= \langle \ln(z_\alpha^{(2)}-x_0)\rangle \boldsymbol{q}_2 && \text{for } y<0 \end{aligned}\right\} \tag{29}$$

The continuity condition on the interface and the condition related to the dislocation give

$$\boldsymbol{q}_1 = \frac{1}{4\pi\mathrm{i}}(\boldsymbol{A}_1-\bar{\boldsymbol{A}}_2\bar{\boldsymbol{B}}_2^{-1}\boldsymbol{B}_1)\boldsymbol{b} \qquad \boldsymbol{q}_2 = -\boldsymbol{B}_2^{-1}\bar{\boldsymbol{B}}_1\bar{\boldsymbol{q}}_1 \tag{30}$$

The corresponding interface traction-charge vector is

$$\boldsymbol{t}(x) = \frac{1}{x-x_0}(\boldsymbol{B}_1\boldsymbol{q}_1+\bar{\boldsymbol{B}}_1\bar{\boldsymbol{q}}_1) = \frac{1}{x-x_0}(\boldsymbol{Y}_*+\bar{\boldsymbol{Y}}_*)\boldsymbol{b} \tag{31}$$

where $\boldsymbol{Y}_* = \dfrac{\boldsymbol{B}_1}{4\pi\mathrm{i}}(\boldsymbol{A}_1-\bar{\boldsymbol{A}}_2\bar{\boldsymbol{B}}_2^{-1}\boldsymbol{B}_1)$.

As was done previously, let

$$\boldsymbol{t}(x) = \frac{1}{x-x_0}(t\boldsymbol{w}+\bar{t}\bar{\boldsymbol{w}}+t_3\boldsymbol{w}_3+t_4\boldsymbol{w}_4) \tag{32}$$

Similarly the related functions $h_i(x)$ are as follows

$$h_1^*(z) = \frac{\bar{\boldsymbol{w}}^{\mathrm{T}}\boldsymbol{H}}{\bar{\boldsymbol{w}}^{\mathrm{T}}\boldsymbol{H}\boldsymbol{w}}\boldsymbol{F}(\varepsilon,\chi,z,x_0,\boldsymbol{I},\boldsymbol{Y}_*+\bar{\boldsymbol{Y}}_*) \tag{33}$$

$$h_2^*(z) = \frac{\boldsymbol{w}^{\mathrm{T}}\boldsymbol{H}}{\boldsymbol{w}^{\mathrm{T}}\boldsymbol{H}\bar{\boldsymbol{w}}}\boldsymbol{F}(-\varepsilon,\bar{\chi},z,x_0,\boldsymbol{I},\boldsymbol{Y}_*+\bar{\boldsymbol{Y}}_*) \tag{34}$$

$$h_3^*(z) = \frac{\boldsymbol{w}_4^{\mathrm{T}}\boldsymbol{H}}{\boldsymbol{w}_4^{\mathrm{T}}\boldsymbol{H}\boldsymbol{w}_3}\boldsymbol{F}(-\mathrm{i}\kappa,\chi_3,z,x_0,\boldsymbol{I},\boldsymbol{Y}_*+\bar{\boldsymbol{Y}}_*) \tag{35}$$

$$h_4^*(z) = \frac{\boldsymbol{w}_3^{\mathrm{T}}\boldsymbol{H}}{\boldsymbol{w}_3^{\mathrm{T}}\boldsymbol{H}\boldsymbol{w}_4}\boldsymbol{F}(\mathrm{i}\kappa,\chi_4,z,x_0,\boldsymbol{I},\boldsymbol{Y}_*+\bar{\boldsymbol{Y}}_*) \tag{36}$$

$$\left.\begin{aligned} c_1 &= -\frac{\bar{\boldsymbol{w}}^{\mathrm{T}}\boldsymbol{H}}{\bar{\boldsymbol{w}}^{\mathrm{T}}\boldsymbol{H}\boldsymbol{w}}\frac{(\boldsymbol{Y}_*+\bar{\boldsymbol{Y}}_*)\boldsymbol{b}}{1+\mathrm{e}^{-2\pi\varepsilon}} && c_2 = -\frac{\boldsymbol{w}^{\mathrm{T}}\boldsymbol{H}}{\boldsymbol{w}^{\mathrm{T}}\boldsymbol{H}\bar{\boldsymbol{w}}}\frac{(\boldsymbol{Y}_*+\bar{\boldsymbol{Y}}_*)\boldsymbol{b}}{1+\mathrm{e}^{2\pi\varepsilon}} \\ c_3 &= -\frac{\boldsymbol{w}_4^{\mathrm{T}}\boldsymbol{H}}{\boldsymbol{w}_4^{\mathrm{T}}\boldsymbol{H}\boldsymbol{w}_3}\frac{(\boldsymbol{Y}_*+\bar{\boldsymbol{Y}}_*)\boldsymbol{b}}{1+\mathrm{e}^{2\mathrm{i}\pi\kappa}} && c_4 = -\frac{\boldsymbol{w}_3^{\mathrm{T}}\boldsymbol{H}}{\boldsymbol{w}_3^{\mathrm{T}}\boldsymbol{H}\boldsymbol{w}_4}\frac{(\boldsymbol{Y}_*+\bar{\boldsymbol{Y}}_*)\boldsymbol{b}}{1+\mathrm{e}^{-2\mathrm{i}\pi\kappa}} \end{aligned}\right\} \tag{37}$$

3 SINGULAR INTEGRAL EQUATIONS

3.1 Electroelastic Fields Induced by Remote Uniform Load

To satisfy the boundary conditions for the branch crack, one needs to know the electroelastic fields induced by the remote uniform load Π_2^∞, as the Green's functions derived above do not satisfy the condition of uniform SED at infinity. In consequence, we set

$$\boldsymbol{f}'(z) = \boldsymbol{f}_0'(z) + \boldsymbol{f}_I'(z) + \boldsymbol{f}_\infty'(z) \tag{38}$$

where $\boldsymbol{f}_\infty(z)$ is the solution corresponding to the remote load. It is convenient to represent the solution due to Π_2^∞ as the sum of a uniform SED in an unflawed solid and a corrective solution in which the main crack is subjected to $-\Pi_2^\infty$. The solution to the latter is[15,18]:

$$\boldsymbol{f}_\infty'(z) = \frac{1}{2}[z(z^2-c^2)^{-1/2} - 1]\boldsymbol{B}^{-1}\Pi_2^\infty \tag{39}$$

for homogeneous material, and

$$\left.\begin{aligned} \boldsymbol{f}_\infty^{\prime(1)}(z) &= \boldsymbol{B}_1^{-1}\left[h_{1\infty}(z)\boldsymbol{w} + h_{2\infty}(z)\bar{\boldsymbol{w}} + h_{3\infty}(z)\boldsymbol{w}_3 + h_{4\infty}(z)\boldsymbol{w}_4\right] \\ \boldsymbol{f}_\infty^{\prime(2)}(z) &= \boldsymbol{B}_2^{-1}\bar{\boldsymbol{H}}^{-1}\boldsymbol{H}\left[h_{1\infty}(z)\boldsymbol{w} + h_{2\infty}(z)\bar{\boldsymbol{w}} + h_{3\infty}(z)\boldsymbol{w}_3 + h_{4\infty}(z)\boldsymbol{w}_4\right] \end{aligned}\right\} \tag{40}$$

for bimaterial, where

$$\left.\begin{aligned} h_{1\infty}(z) &= \frac{1}{1+\mathrm{e}^{-2\pi\varepsilon}}\left[\left(\frac{z-c}{z+c}\right)^{\mathrm{i}\varepsilon}(z^2-c^2)^{-1/2}(z+2\mathrm{i}c\varepsilon) - 1\right]\frac{\bar{\boldsymbol{w}}^{\mathrm{T}}\boldsymbol{H}\Pi_2^\infty}{\bar{\boldsymbol{w}}^{\mathrm{T}}\boldsymbol{H}\boldsymbol{w}} \\ h_{2\infty}(z) &= \frac{1}{1+\mathrm{e}^{2\pi\varepsilon}}\left[\left(\frac{z-c}{z+c}\right)^{-\mathrm{i}\varepsilon}(z^2-c^2)^{-1/2}(z-2\mathrm{i}c\varepsilon) - 1\right]\frac{\boldsymbol{w}^{\mathrm{T}}\boldsymbol{H}\Pi_2^\infty}{\boldsymbol{w}^{\mathrm{T}}\boldsymbol{H}\bar{\boldsymbol{w}}} \\ h_{3\infty}(z) &= \frac{1}{1+\mathrm{e}^{2\pi\mathrm{i}\kappa}}\left[\left(\frac{z-c}{z+c}\right)^{\kappa}(z^2-c^2)^{-1/2}(z+2\kappa c) - 1\right]\frac{\boldsymbol{w}_4^{\mathrm{T}}\boldsymbol{H}\Pi_2^\infty}{\boldsymbol{w}_4^{\mathrm{T}}\boldsymbol{H}\boldsymbol{w}_3} \\ h_{4\infty}(z) &= \frac{1}{1+\mathrm{e}^{-2\pi\mathrm{i}\kappa}}\left[\left(\frac{z-c}{z+c}\right)^{-\kappa}(z^2-c^2)^{-1/2}(z-2\kappa c) - 1\right]\frac{\boldsymbol{w}_3^{\mathrm{T}}\boldsymbol{H}\Pi_2^\infty}{\boldsymbol{w}_3^{\mathrm{T}}\boldsymbol{H}\boldsymbol{w}_4} \end{aligned}\right\} \tag{41}$$

So far the function $\boldsymbol{f}(z)$ satisfies the conditions at infinity and on the main crack face. It remains only to make sure that the traction-charge free conditions for the branch crack are met.

3.2 Singular Integral Equations and Solution Methods

The remaining boundary conditions for the branch can be satisfied by redefining the discrete dislocation $\boldsymbol{b}$, in terms of distributed dislocation densities, $\boldsymbol{b}(\xi)$ defining along the line, $z = c + \eta z^*$, $z_0 = c + \xi z^*$, where $z^* = \cos\theta + p\sin\theta$ emanating from the main crack tip. For simplicity we first consider the case of a branch in a homogeneous solid. Enforcing the satisfaction of traction-charge free condition on the branch, a system of singular integral equations for the dislocation $\boldsymbol{b}(\xi)$ is obtained as

$$\frac{\boldsymbol{L}}{2\pi}\int_0^a \frac{\boldsymbol{b}(\xi)\mathrm{d}\xi}{\eta-\xi} + \frac{1}{\pi}\int_0^a \boldsymbol{Y}_0(\eta,\xi)\boldsymbol{b}(\xi)\mathrm{d}\xi + \boldsymbol{Q}_\infty(\eta) = 0 \tag{42}$$

where $\boldsymbol{Y}_0(\eta,\xi)$ is a kernel matrix function of the singular integral equation and is Holder-continuous along $0 \le \xi \le a$, $\boldsymbol{Q}_\infty(\eta)$ is a known function vector corresponding to the SED field induced by the external load. They are

$$\boldsymbol{Y}_0(\eta,\xi) = \mathrm{Im}\{\bar{\boldsymbol{B}}\langle z_\alpha^*\rangle\boldsymbol{F}_*(z,\bar{z}_0)\bar{\boldsymbol{B}}^{\mathrm{T}} - \boldsymbol{B}\langle z_\alpha^*\rangle\boldsymbol{F}_*(z,z_0)\boldsymbol{B}^{\mathrm{T}}\} \tag{43}$$

$$Q_\infty(\eta) = \mathrm{Re}\Big\{B\Big\langle z_\alpha^*\Big[\frac{z_\alpha}{(z_\alpha^2 - c^2)^{1/2}} - 1\Big]\Big\rangle B^{-1}\Pi_2^\infty\Big\} \tag{44}$$

in which $z_\alpha^* = \cos\theta + p_\alpha \sin\theta$.

For the purpose of numerical solution, the following normalized quantities are introduced

$$s_0 = \frac{2\eta - a}{a} \qquad s = \frac{2\xi - a}{a} \tag{45}$$

If we retain the same symbols for the new functions caused by the change of the variables, the singular integral equation (42) can, then, be rewritten in the form

$$\frac{L}{2\pi}\int_{-1}^{1}\frac{b(s)\mathrm{d}s}{s_0 - s} + \frac{1}{\pi}\int_{-1}^{1} Y_0(s, s_0)b(s)\mathrm{d}s + Q_\infty(s_0) = 0 \tag{46}$$

Similarly for a branch in a bimaterial solid, the corresponding singular equation can be obtained as

$$\frac{L_1}{2\pi}\int_{-1}^{1}\frac{b(s)\mathrm{d}s}{s_0 - s} + \frac{1}{\pi}\int_{-1}^{1}\{Y_0(s, s_0)b(s) + Y_1(s, s_0)\}\mathrm{d}s + Q_\infty(s_0) = 0 \tag{47}$$

where

$$Y_0(s, s_0) = \mathrm{Im}\Big\{B_1\sum_{k=1}^{4}\Big\langle\frac{z_\alpha^{(1)^*}}{(s_0+1)z_\alpha^{(1)^*} - (s+1)\bar{z}_k^{(1)^*}}\Big\rangle B^* I_k \bar{B}_1^{\mathrm{T}} \tag{48}$$

$$Y_1(s, s_0) = \pi a \mathrm{Re}\Big\{B_1\langle z_\alpha^{(1)^*}\rangle B_1^{-1} h(s, s_0)\Big\} \tag{49}$$

$$Q_\infty(s, s_0) = 2\mathrm{Re}\{B_1\langle z_\alpha^{(1)^*}\rangle f_\infty^{(1)}(s, s_0)\} \tag{50}$$

3.3 Numerical Scheme

Both the integral equations (46) and (47) can be solved numerically using a method developed by Erdogan and Gupta[22]. First we write the unknown density function, $b(s)$ in Eq.(46) in the form[7]

$$b(s) = \frac{\hat{b}(s)}{\sqrt{1-s^2}} = \frac{\sum_{j=1}^{m}\hat{b}_j T_j(s)}{\sqrt{1-s^2}} \tag{51}$$

where $\hat{b}(s)$ is a regular function vector defined in the interval $|s| \le 1$, and $\hat{b}(-1) = 0$[7], since the SED behaves like $d^{-1/2}$, here d measures distance from the branched crack tip, and the SED at the vertex behaves as $d^{-\varepsilon}$, $(\varepsilon < 1/2)$ for a SED-free wedge with a wedge angle less than π. $\hat{b}_j$ are the real unknown constant vectors, and $T_j(s)$ the Chebyshev polynomials of first kind. Thus the discretized form of Eq.(46) (or Eq.(47)) together with the condition, $\hat{b}(-1) = 0$, may be written as[22]

$$\left.\begin{aligned}&\sum_{k=1}^{m}\frac{1}{n}\Big[\frac{L}{2(s_{0r} - s_k)} + Y_0(s_{0r}, s_k)\Big]\hat{b}(s_k) + Q_\infty(s_{0r}) = 0\\ &\sum_{k=1}^{m}\hat{b}_k(-1) = 0\end{aligned}\right\} \tag{52}$$

for a homogeneous solid, and

$$\left.\begin{aligned}&\sum_{k=1}^{m}\frac{1}{n}\Big\{\Big[\frac{\boldsymbol{L}_1}{2(s_{0r}-s_k)}+\boldsymbol{Y}_0(s_{0r},s_k)\Big]\hat{\boldsymbol{b}}(s_k)+\hat{\boldsymbol{Y}}_1(s_{0r},s_k)\Big\}+\boldsymbol{Q}_\infty(s_{0r})=0\\&\sum_{k=1}^{m}\hat{\boldsymbol{b}}_k(-1)=0\end{aligned}\right\}\tag{53}$$

for a bimaterial solid, where

$$\boldsymbol{Y}_1(x,y)=\frac{\hat{\boldsymbol{Y}}_1(x,y)}{\sqrt{1-s^2}}\tag{54}$$

$$\left.\begin{aligned}&s_k=\cos\Big[\frac{(2k-1)\pi}{2m}\Big] && (k=1,2,\cdots,m)\\&s_{0r}=\cos\Big(\frac{r\pi}{m}\Big) && (r=1,2,\cdots,m-1)\end{aligned}\right\}\tag{55}$$

Equation (52) (or Eq.(53)) provides a system of $4m$ equations for the determination of the $4m$-values $\hat{b}_{kj}$. Once the function $\hat{\boldsymbol{b}}(s)$ has been found from Eq.(52), the SED, $\Pi_n^{(1)}(\eta)$, in a coordinate local to the crack branch line can be expressed in the form

$$\Pi_n^{(1)}(s_0)=\Omega(\theta)\Big[\frac{\boldsymbol{L}}{2\pi}\int_{-1}^{1}\frac{\boldsymbol{b}(s)}{s_0-s}\mathrm{d}s+\int_{-1}^{1}\boldsymbol{Y}_0(s,s_0)\boldsymbol{b}(s)\mathrm{d}s+\boldsymbol{Q}_\infty(s_0)\Big]\tag{56}$$

for a homogeneous solid, and

$$\Pi_n^{(1)}(s_0)=\Omega(\theta)\Big[\frac{\boldsymbol{L}_1}{2\pi}\int_{-1}^{1}\frac{\boldsymbol{b}(s)\mathrm{d}s}{s_0-s}+\frac{1}{\pi}\int_{-1}^{1}\{\boldsymbol{Y}_0(s,s_0)\boldsymbol{b}(s)+\boldsymbol{Y}_1(s,s_0)\}\mathrm{d}s+\boldsymbol{Q}_\infty(s_0)\Big]\tag{57}$$

for a bimaterial solid, where the 4×4 matrix $\Omega(\theta)$ whose components are the cosine of the angle between the local coordinates and the global coordinates is in the form

$$\Omega(\theta)=\begin{bmatrix}\cos\theta & \sin\theta & 0 & 0\\ -\sin\theta & \cos\theta & 0 & 0\\ 0 & 0 & 1 & 0\\ 0 & 0 & 0 & 1\end{bmatrix}\tag{58}$$

4 SED INTENSITY FACTORS AND ENERGY RELEASE RATE

The SED intensity factors at the right tip of the branch crack are of interest and can be derived by first considering the traction and surface charge (TSC) on the direction of the branch line and considering the TSC very near the tip ($s\to 1$) which is given by Eq.(54)

$$\Pi_n^{(1)}(r)\approx\Omega(\theta)\frac{\boldsymbol{L}^*\hat{\boldsymbol{b}}(1)}{\sqrt{8(s-1)}}=\frac{1}{4}\sqrt{a/r}\,\Omega(\theta)\boldsymbol{L}^*\hat{\boldsymbol{b}}(1)\tag{59}$$

where r is a distance ahead of the branch tip, $\boldsymbol{L}^*=\boldsymbol{L}$ for a homogeneous material, and $\boldsymbol{L}^*=\boldsymbol{L}_1$ for a bimaterial.

Using Eq.(59) we can calculate the SED intensity factors at the right tip of the branch by the following usual definition

$$\boldsymbol{K} = \{K_{\mathrm{II}}\ K_{\mathrm{I}}\ K_{\mathrm{III}}\ K_D\}^{\mathrm{T}} = \lim_{r\to 0}\sqrt{2\pi r}\Pi_n^{(1)}(r) \tag{60}$$

Combining with the results of Eq.(59), one then leads to

$$\boldsymbol{K} \approx \sqrt{a\pi/8}\,\Omega(\theta)\boldsymbol{L}^*\hat{\boldsymbol{b}}(1) \tag{61}$$

Thus the solution of the singular integral equation enables the direct determination of the stress intensity factors.

The energy release rate G can be computed by the closure integral[23]

$$G = \lim_{x\to 0}\frac{1}{2x}\int_0^x \Pi_n^{(1)\mathrm{T}}(r)\Delta\boldsymbol{u}_n(x-r)\mathrm{d}r \tag{62}$$

where x is the assumed crack extension, $\Delta\boldsymbol{u}$ is a vector of elastic displacement and electric potential jump across the branch crack. Noting that

$$\Delta\boldsymbol{u}(\eta) = \int_a^\eta \boldsymbol{b}(\xi)\mathrm{d}\xi \tag{63}$$

we have

$$G = \lim_{x\to 0}\frac{1}{2x}\int_0^x \Phi_n^{(1)\mathrm{T}}(r)\frac{\partial\Delta\boldsymbol{u}_n(x-r)}{\partial x}\mathrm{d}r \tag{64}$$

where

$$\Phi_n^{(1)}(r) = \int^r \Pi_n^{(1)}(x)\mathrm{d}x \tag{65}$$

During the derivation of Eq.(64), the following conditions have been employed

$$\Phi_n^{(1)}(0) = 0 \qquad \Delta\boldsymbol{u}(x-r)|_{r=x} = 0 \tag{66}$$

Substituting Eq.(51) into (63), and Eq.(59) into (65), then into Eq.(64), one obtains

$$G = \frac{a\pi}{16}\hat{\boldsymbol{b}}^{\mathrm{T}}(1)\boldsymbol{L}^*[\Omega^{\mathrm{T}}(\theta)]^2\hat{\boldsymbol{b}}(1) \tag{67}$$

5 CRITERION FOR CRACK KINKING

An interface crack can advance either by continuing growth in the interface or by kinking out of the interface into one of the adjoining materials. This competition can be assessed by comparing the ratio of the energy release rate for kinking out of the interface and for interface cracking, G_{kink}/G_i, to the ratio of substrate toughness to interface toughness, Γ_s/Γ_i. In effect, if

$$\frac{G_{\mathrm{kink}}}{G_i} > \frac{\Gamma_s}{\Gamma_i} \tag{68}$$

kinking is favoured. Conversely, if the inequality in Eq.(68) is reversed, the flaw meets the condition for continuing advance in the interface at an applied load lower than that necessary to advance the crack into the substrate, where Γ_s and Γ_i are substrate and interface toughness, respectively. For a given load condition, Π_2^∞, the fracture toughness, Γ, is defined

as the energy release rate G at the onset of the crack growth and has discussed in detail elsewhere[9]. G_{kink} and G_i are the energy release rates for kinking out of the interface and for interface cracking, respectively, in which G_i can be derived by setting $\theta = 0$ in the previous sections, and G_{kink} is related to SED intensity factors, $\boldsymbol{K}$, by

$$G_{\text{kink}} = \frac{1}{2}\boldsymbol{K}\boldsymbol{D}\boldsymbol{K} \tag{69}$$

where $\boldsymbol{D} = \Omega^{\mathrm{T}}(\theta)\boldsymbol{L}^{*-1}\Omega^{\mathrm{T}}(\theta)$.

6 NUMERICAL RESULTS

As numerical illustration of the proposed formulation, we consider a piezoelectric bimaterial plate with an interface crack of length $2c$, a branch crack of length a and its interface coincided with x_1-axis as shown in Fig.1. In all following calculations, the ratio of a/c is taken to be 0.1. The upper and lower materials are assumed to be PZT-5H and PZT-5[24], respectively. The material constants for the two materials are as follows:

(1) material properties for PZT-5H:

$c_{11} = 117\,\text{GPa}$, $c_{12} = c_{13} = 53\,\text{GPa}$, $c_{22} = c_{33} = 126\,\text{GPa}$, $c_{44} = 35.5\,\text{GPa}$,

$C_{23} = 55\,\text{GPa}$, $c_{55} = c_{66} = 35.3\,\text{GPa}$, $e_{12} = e_{13} = -6.5\,\text{C/m}^2$, $e_{11} = 23.3\,\text{C/m}^2$,

$e_{35} = e_{26} = 17\,\text{C/m}^2$, $\kappa_{11} = 130 \times 10^{-10}\,\text{C/Vm}$, $\kappa_{22} = \kappa_{33} = 151 \times 10^{-10}\,\text{C/Vm}$

(2) material properties for PZT-5:

$c_{11} = 111\,\text{GPa}$, $c_{12} = c_{13} = 75.2\,\text{GPa}$, $c_{22} = c_{33} = 121\,\text{GPa}$, $c_{44} = 22.8\,\text{GPa}$,

$C_{23} = 75.4\,\text{GPa}$, $c_{55} = c_{66} = 21.1\,\text{GPa}$, $e_{12} = e_{13} = -5.4\,\text{C/m}^2$, $e_{11} = 15.8\,\text{C/m}^2$,

$e_{35} = e_{26} = 12.3\,\text{C/m}^2$, $\kappa_{11} = 73.46 \times 10^{-10}\,\text{C/Vm}$, $\kappa_{22} = \kappa_{33} = 81.7 \times 10^{-10}\,\text{C/Vm}$

The ratio G_{kink}/G_i versus kink angle θ with $\sigma_{13}^{\infty} = D_2^{\infty} = 0$ are shown in Fig.2 for a number of loading combinations measured by $\psi = \tan^{-1}(K_{\text{II}}^{\infty}/K_{\text{I}}^{\infty})$, where K_{I} and K_{II} are the conventional mode I and mode II stress intensity factors. The curve clearly shows that the maximum energy release rate occurs at different kink angle $\hat{\theta}$ for different loading phase ψ, where $\hat{\theta}$ is the critical kink angle for which the maximum energy release rate will occur under a given loading condition. For example, $\hat{\theta} = 0°$ for curves 4 and 5, $\hat{\theta} = 11°$ for curve 3, $\hat{\theta} = 13°$ for curve 4 and $\hat{\theta} = 18°$ for curve 1.

The ratio of G_{kink}/G_i is plotted in Fig.3 as a function of kink angle θ for several values of remote loading D_2^{∞} with $\sigma_{11}^{\infty} = 4 \times 10^6\,\text{N/m}^2$ and $\sigma_{12}^{\infty} = \sigma_{13}^{\infty} = 0$. The calculation indicates that the energy release rate can have negative value depending on the direction and magnitude of the remote loading D_2^{∞}. For this particular problem, the energy release rate G_i will be positive when $-1.8 \times 10^{-3}\,\text{C/m}^2 < D_2^{\infty} < 1.8 \times 10^{-3}\,\text{C/m}^2$. Figure 3 also shows that the critical kink angle is affected by the load D_2^{∞}. Generally, the critical kink angle will increase along with the increase of absolute value of D_2^{∞}.

Figure 4 shows the variation of G_{kink}/G_0 as a function of D_2^{∞} for several values of kink angle θ and again for $\sigma_{11}^{\infty} = 4 \times 10^6\,\text{N/m}^2$ and $\sigma_{12}^{\infty} = \sigma_{13}^{\infty} = 0$. Here G_0 is the value of G at zero electric loads. It can be seen from this figure that the ratio of G_{kink}/G_0 will mostly decrease along with the increase of the magnitude of electric load.

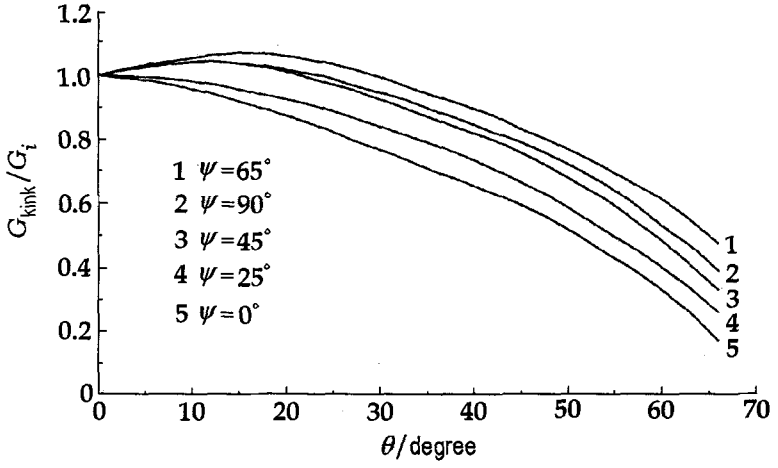

Fig.2 Variation of G_{kink}/G_i with kink angle θ for several loading combinations specified by $\psi = \tan^{-1}(K_{\text{II}}/K_{\text{I}})$

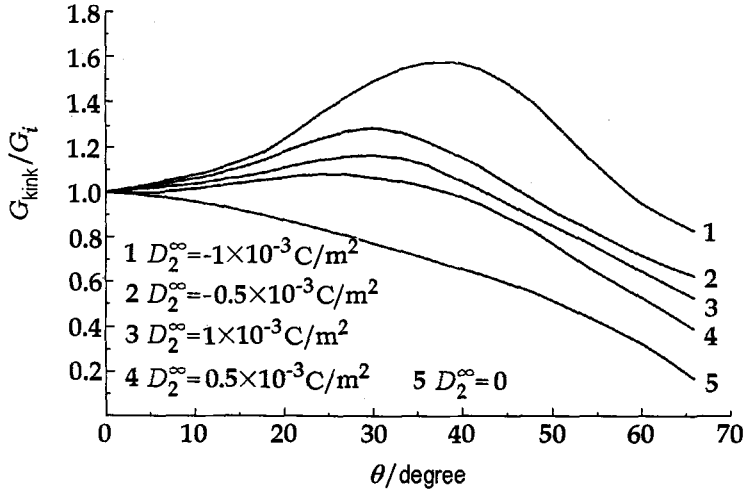

Fig.3 Variation of G_{kink}/G_i with kink angle θ for several loadings $D_2^\infty(\sigma_{11}^\infty = 4 \times 10^6\,\text{N/m}^2)$

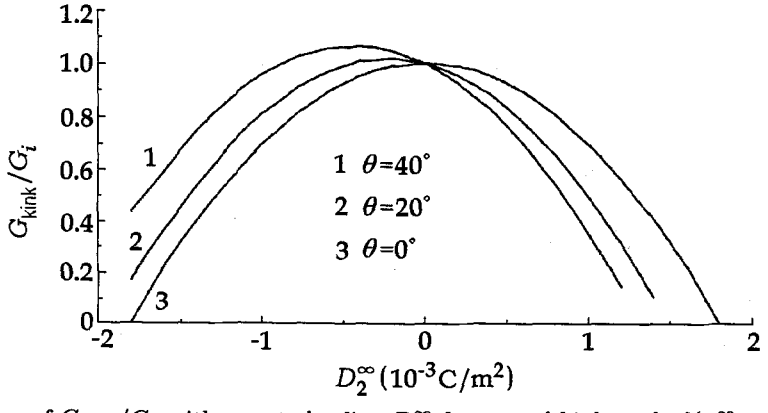

Fig.4 Variation of G_{kink}/G_0 with remote loading D_2^∞ for several kink angle $\theta(\sigma_{11}^\infty = 4 \times 10^6\,\text{N/m}^2)$

7 CONCLUSIONS

An integral equation solution has been presented for determining whether cracks extend along, or kink out of interface between two piezoelectric materials. In this investigation, explicit Green's function for an interface crack subject to an edge dislocation is derived allowing a branched crack problem to be expressed in terms of coupled singular integral equations. The resulting integral equations involve the dislocation density function defined on the line of branch only. As a result, the formulation for the energy release rate and SED intensity factors can be expressed in terms of the dislocation density function and the branch angle. A particular example of a bimaterial containing an interface crack and a branch was examined to see the application of the proposed formulation. By way of the maximum energy release rate criterion, the numerical solution developed can be used to assess whether an interface crack will extend in the interface or whether it will kink out of the interface. The analysis also shows that the energy release rate can have either positive or negative values in the presence of electric load, depending on the direction and the magnitude of the applied electric displacement. In other words, for a given mechanical load, presence of the applied electric displacement can either promote or retard crack extension. This conclusion may be useful in designing piezoelectric components with interface.

REFERENCES

1 Evans AG, Dalgleish BJ, He MY, Hutchinson JW. On crack path selection and the interface fracture energy in bimaterial systems. *Acta Metall*, 1989, 37: 3249~3254

2 Sih GC. Strain energy factors applied to mixed mode crack problems. *Int J Frac*, 1974, 10: 305~321

3 Hayashi K, Nemat-Nasser S. Energy-release rate and crack kinking under combined loading. *Journal of Applied Mechanics*, 1981, 48: 520~524

4 He MY, Evans AG, Hutchinson JW. Interface cracking phenomena in constrained metal layers. *Acta Materialia*, 1996, 44: 2963~2971

5 Lo KK. Analysis of branched cracks. *Journal of Applied Mechanics*, 1978, 45: 797~802

6 Hayashi K, Nemat-Nasser S. On branched, interface cracks. *Journal of Applied Mechanics*, 1981, 48: 529~533

7 He MY, Hutchinson JW. Kinking of a crack out of an interface. *Journal of Applied Mechanics*, 1989, 56: 270~278

8 Miller GR, Stock WL. Analysis of branched interface cracks between dissimilar anisotropic media. *Journal of Applied Mechanics*, 1989, 56: 844~849

9 Hutchinson JW, Suo Z. Mixed mode cracking in layered materials. In: Hutchinson JW, Wu TY eds, *Advances in Applied Mechanics*, 1992, 29: 63~191

10 Wang TC, Shih CF, Suo Z. Crack extension and kinking in laminates and bicrystals. *Int J Solids Struct*, 1992, 29: 327~344

11 Atkinson C, Bastero C, Sanchez MI. Prediction of branching (or relaxation) angle in anisotropic or isotropic elastic bimaterials with rigid substrate. *Int J Frac*, 1994, 67: 231~261

12 Stroh AN. Dislocations and cracks in anisotropic elasticity. *Phil Mag*, 1958, 7: 625~646

13 Barnett DM, Lothe J. Dislocations and line charges in anisotropic piezoelectric insulators. *Phys Stat Sol* (b), 1975, 67: 105~111

14 Chung MY, Ting TCT. Piezoelectric solid with an elliptic inclusion or hole. *Int J Solids Struct*, 1996, 33: 3343~3361

15 Yu SW, Qin QH. Damage analysis of thermopiezoelectric properties: Part I—crack tip singularities. *Theoretical and Applied Fracture Mechanics*, 1996, 25: 263~277

16 Qin QH. A new solution for thermopiezoelectric solid with an insulated elliptic hole. *Acta Mechanica Sinica*, 1998, 14: 157~170

17 Suo Z. Singularities, interfaces and cracks in dissimilar anisotropic media. *Proc R Soc Lond*, 1990, A427: 331~358

18 Suo Z, Kuo CM, Barnett DM, Willis JR. Fracture mechanics for piezoelectric ceramics. *J Mech Phys Solids*, 1992, 40: 739~765

19 Qin QH, Mai YW. Crack growth prediction of an inclined crack in a half-plane thermopiezoelectric solid. *Theoretical and Applied Fracture Mechanics*, 1997: 26: 185~191

20 Muskhelishvili NI. Some Basic Problems of Mathematical Theory of Elasticity. Groningen, Holland: NVP Noordhoff Ltd, 1953

21 Qin QH, Mai YW. Thermoelectroelastic Green's function and its application for bimaterial of piezoelectric materials. *Archive of Applied Mechanics*, 1998, 68: 433~444

22 Erdogan F, Gupta GD. On the numerical solution of singular integral equations. *Q Appl Mathe*, 1972, 32: 525~534

23 Park SB, Sun CT. Effect of electric field on fracture of piezoelectric ceramics. *Int J Frac*, 1995, 70: 203~216

24 Qin QH, Yu SW. An arbitrarily-oriented plane crack terminating at the interface between dissimilar piezoelectric materials. *Int J Solids Struct*, 1997, 34: 581~590